Geological Society of America Bulletin

Controls on large landslide distribution and implications for the geomorphic evolution of the southern interior Columbia River basin

Elizabeth B. Safran, Scott W. Anderson, Megan Mills-Novoa, P. Kyle House and Lisa Ely

Geological Society of America Bulletin 2011;123, no. 9-10;1851-1862
doi: 10.1130/B30061.1

Controls on large landslide distribution and implications for the geomorphic evolution of the southern interior Columbia River basin

Elizabeth B. Safran[1]*, Scott W. Anderson[2†], Megan Mills-Novoa[1], P. Kyle House[3§], and Lisa Ely[4]
[1]*Environmental Studies Program, Lewis & Clark College, Portland, Oregon 97219, USA*
[2]*Physics Department, Lewis & Clark College, Portland, Oregon 97219, USA*
[3]*Nevada Bureau of Mines and Geology and University of Nevada at Reno, Reno, Nevada 89503, USA*
[4]*Department of Geological Sciences, Central Washington University, Ellensburg, Washington 98926, USA*

ABSTRACT

Large landslides (>0.1 km^2) are important agents of geomorphic change. While most common in rugged mountain ranges, large landslides can also be widespread in relatively low-relief (several 100 m) terrain, where their distribution has been relatively little studied. A fuller understanding of the role of large landslides in landscape evolution requires addressing this gap, since the distribution of large landslides may affect broad regions through interactions with channel processes, and since the dominant controls on landslide distribution might be expected to vary with tectonic setting. We documented >400 landslides between 0.1 and ~40 km^2 across ~140,000 km^2 of eastern Oregon, in the semiarid, southern interior Columbia River basin. The mapped landslides cluster in a NW-SE–trending band that is 50–100 km wide. Landslides predominantly occur where even modest local relief (~100 m) exists near key contacts between weak sedimentary or volcaniclastic rock and coherent cap rock. Fault density exerts no control on landslide distribution, while ~10% of mapped landslides cluster within 3–10 km of mapped fold axes. Landslide occurrence is curtailed to the NE by thick packages of coherent basalt and to the SW by limited local relief. Our results suggest that future mass movements will localize in areas stratigraphically preconditioned for landsliding by a geologic history of fluviolacustrine and volcaniclastic sedimentation and episodic capping by coherent lava flows. In such areas, episodic landsliding may persist for hundreds of thousands of years or more, producing valley wall slopes of ~7°–13° and impacting local channels with an evolving array of mass movement styles.

INTRODUCTION

Large landslides are important agents of geomorphic change, capable of shaping ridge morphology (e.g., Roering et al., 2005), delivering sediment to channels (e.g., Hovius et al., 1997), shifting drainage divides (e.g., Hasbargen and Paola, 2000; Mather et al., 2003), promoting drainage integration (e.g., Hovius et al., 1998), and damming rivers (e.g., Costa and Schuster, 1988). The role that large landslides can play in the spatial-temporal evolution of a particular landscape depends partly on the dominant controls on landslide occurrence. Analysis of the spatial distribution of landslide populations is a useful approach to identifying these controls because it incorporates many instances of landsliding at once.

Most studies of large landslide populations have centered on rugged, mountainous terrain. Korup et al. (2007) analyzed 300 giant landslides and showed that two thirds of them occurred on the steepest 5% of the global landscape. Such landscapes are typically convergent zones dominated by rock avalanches or giant rock flows (e.g., Hermanns and Strecker, 1999; Korup et al., 2006; Antinao and Gosse, 2008). However, giant landslides also occur in regions of only several hundred meters of local relief (Korup et al., 2007; Philip and Ritz, 1999; Reneau and Dethier, 1996), characteristic of continental interiors. Relatively few studies have focused on landslide populations and controls on their distribution in these low-relief zones. A fuller understanding of the role of large landslides in landscape evolution requires addressing this gap, since the dominant controls on landslide distribution might be expected to vary with tectonic setting, and since the distribution of large landslides may affect both interfluve character and channel processes, thus impacting broad regions.

In this study, we mapped and analyzed the distribution of over 400 large (arbitrarily defined as >0.1 km^2 in areal extent) landslides in the semiarid uplifted volcanic plateaus of the southern interior Columbia River basin (Fig. 1), motivated by reports of large landslides at several localities in the region (e.g., Plumley, 1986; Badger and Watters, 2004; Beebee, 2003; O'Connor et al., 2003; Othus, 2008). While topographic gradients ultimately drive mass movement, anecdotal observations (Beebee, 2003) and limit-equilibrium stability analyses (Badger and Watters, 2004) suggest that lithologic and stratigraphic controls may promote large landslides in our study area. There, coherent volcanic rock commonly caps weak volcaniclastic debris and/or fluviolacustrine sediments. Such conditions reflect the relatively dry, predominantly extensional, backarc setting where trunk streams may be tectonically or volcanically disrupted, forming low-gradient depocenters (e.g., Smith, 1986a; Cummings et al., 2000) in which sediments may subsequently be mantled with effusive lava flows. Stratigraphic controls on landsliding have been widely cited in the literature (e.g., Rib and Liang, 1978; Crozier, 2010) and have proven important in other relatively low-relief settings, such as along the Rio Grande valley of New Mexico (Reneau and Dethier, 1996) or the Columbia River Gorge between Oregon and Washington (Palmer, 1977). However, tectonic structures themselves and associated seismic accelerations can also localize landslides in relatively low-relief settings (e.g., Philip and Ritz, 1999; Badger and Watters, 2004), as well as in more rugged landscapes (e.g., Antinao and Gosse, 2008).

This paper investigates the relative influences of lithologic, topographic, and structural controls

*E-mail: safran@lclark.edu
†Current address: Department of Geography, University of Colorado at Boulder, Boulder, Colorado 80309, USA.
§Current address: U.S. Geological Survey, Flagstaff, Arizona 86001, USA.

GSA Bulletin; September/October 2011; v. 123; no. 9/10; p. 1851–1862; doi: 10.1130/B30061.1; 14 figures; 1 table; Data Repository item 2011017.

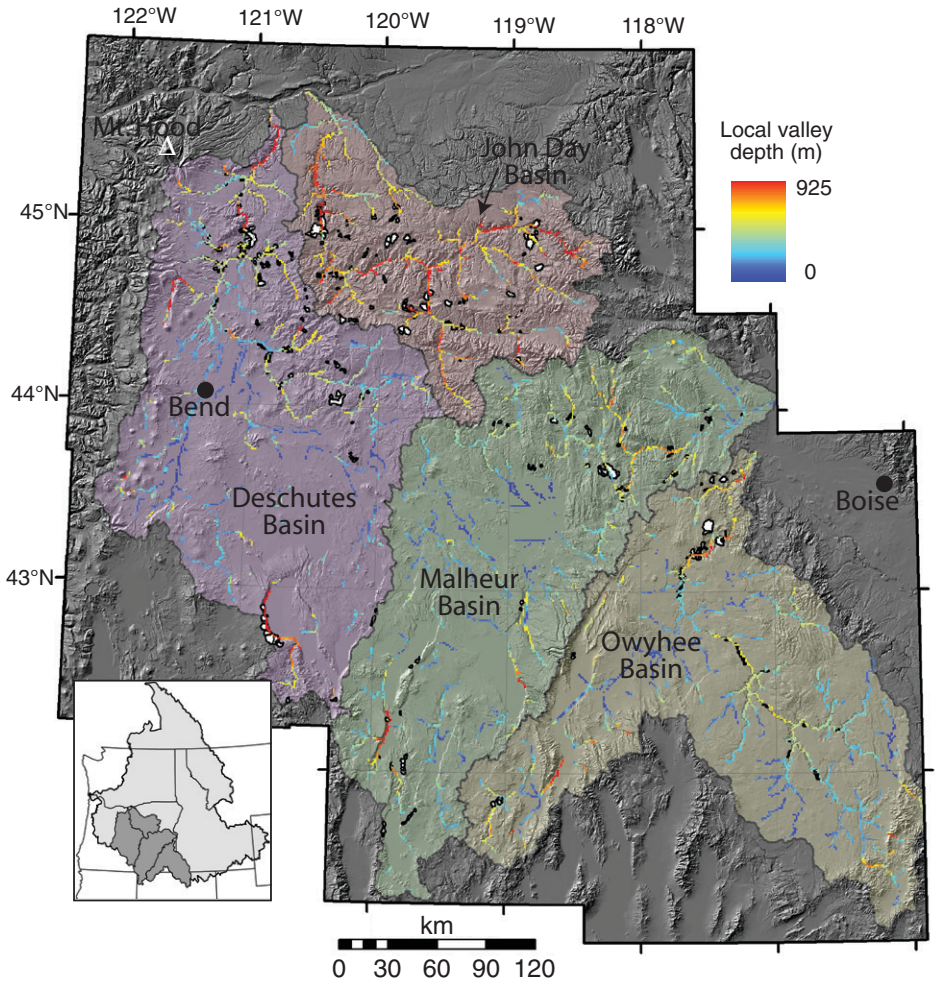

Figure 1. Distribution of large landslides in the study region. Landslides are shown in white and are superimposed on shaded relief image. Channel network derived from ArcGIS is shown in blue to red spectrum; color represents local valley depth, defined as maximum difference in elevation within a circle 4 km in diameter from a given point on the channel network. Pixels in the channel network are enlarged to 1 km on a side for visibility. Channel network derived from digital elevation model (DEM) over-represents true drainage density in southern portion of study area. Inset shows study area relative to Columbia River basin.

on landslide distribution in an extensive, low-relief setting using spatial analyses supplemented by select field observations. Specifically, we assess how widespread large landslides are in the region; which controls most strongly govern their distribution; and what those controls imply about future landscape evolution in the study area, particularly as mediated by hillslope-channel interactions (e.g., Palmquist and Bible, 1980; Korup et al., 2010).

STUDY AREA

Our landslide mapping and geospatial analyses were centered on the southern part of the interior Columbia River basin, an area of ~140,000 km^2 including the Deschutes (40,600 km^2), John Day (20,500 km^2), Malheur (40,800 km^2), and Owyhee (36,500 km^2) River basins (Fig. 1). Basin designations derive from geospatial routines that fill closed depressions. They therefore include areas in the river basins that are presently internally drained, some of which were integrated during wetter climatic periods (e.g., Carter et al., 2006). These areas were intentionally included to broaden the range of landscape character analyzed. The study area is geologically varied enough to offer general lessons about controls on landslide distribution but limited enough to make geospatial analysis manageable.

The region is characterized by a semiarid climate. Average annual precipitation is predominantly 25–38 cm/yr, with local maxima of 50–75 cm/yr in the Ochoco and Strawberry Mountains. Precipitation reaches 300 cm/yr at points along the western border of the Deschutes River basin, which lies in permeable, young volcanic rocks of the Cascade Range, giving this river a much more uniform flow regime than that of other regional rivers (O'Connor and Grant, 2003).

Extensive portions of the study area have accumulated eruptive products from arc-type volcanism over the last ~55 m.y. (Christiansen and Yeats, 1992), creating such regionally significant units as the John Day and Clarno Formations. Many of the basins in which volcaniclastic and fluviolacustrine sediments accumulated are tectonically controlled, reflecting regional extension beginning in the Miocene (Cummings, 1991; Christiansen and Yeats, 1992; Cummings et al., 2000). The southern portion of the study area was affected by Miocene-Pliocene Basin and Range–style extension (Plumley, 1986; Evans, 1987; Malde, 1991; Ferns et al., 1993; Christiansen and Yeats, 1992; Orr and Orr, 1999). The Miocene Columbia River Basalt Group is exposed in the lower reaches of the Deschutes and John Day Rivers in the northern portion of the study area. The southeastern portion is also underpinned by Columbia River Basalt Group equivalents (Camp and Ross, 2004) that are buried by younger volcanic, volcaniclastic, and fluvial or fluviolacustrine units. The study region experienced northwestward propagation of bimodal volcanism from the McDermitt caldera complex to Newberry volcano from the Miocene to the Holocene (Christiansen and Yeats, 1992; Jordan et al., 2004). Dissection of resistant rhyolitic units has produced some of the most impressive fluvial canyons in the region (e.g., on the Owyhee and Deschutes Rivers).

Elevations throughout the region are largely >1 km above sea level (asl), with an average surface elevation of almost 1.4 km asl near the convergence of the Oregon-Idaho-Nevada borders (Camp and Ross, 2004). This topographic high may be in part thermally controlled, reflecting the localization and persistence of a sheared-off mantle plume head associated with eruption of the Columbia River Basalt Group (Camp and Ross, 2004). Although most basic drainage directions were established regionally from middle Miocene to early Pliocene times (e.g., Smith, 1986a; Beranek et al., 2006), the incised, modern river system was likely not established until mid- to late Pliocene. Paleontological and stratigraphic evidence suggests the Columbia River captured the Snake River system ca. 3–4 Ma (Van Tassell et al., 2001; Repenning et al., 1995), but subsequent incision of Hell's Canyon may have been relatively slow (Wood and Clemens, 2002). These events directly

affected the Malheur and Owyhee Rivers, both tributaries to the Snake River. The Deschutes River occupied a broad plain several hundred meters above its current level until ca. 4 Ma and did not occupy a canyon near present-day elevations until 1.2 Ma (Smith, 1986b).

LANDSLIDE DISTRIBUTION AND POPULATION

Although many landslides have been recognized and mapped in parts of the study area, the criteria for delineating these features on small-scale maps (e.g., Walker and MacLeod, 1991) are not always clear. In compilations of larger-scale maps (e.g., Burns et al., 2008; Ma et al., 2009), these criteria vary. We created our own landslide map based on uniform criteria in the Deschutes, John Day, Malheur, and Owyhee River basins, using: (1) shaded relief renderings of 10 m digital elevation models (DEMs) assembled from the National Elevation Data set (NED); (2) digital raster graphics (DRGs) representing U.S. Geological Survey (USGS) 7.5′ topographic quadrangles; (3) 1-m-resolution color digital orthophoto quarter quadrangles (DOQQs) from the National Agriculture Imagery Program; and (4) Google Earth imagery. ArcMap and Google Earth were both used for viewing and superimposing imagery.

Landslides were identified on the basis of one or more of the following criteria: (1) distinct, often scalloped, headscarps; (2) hummocky terrain, texturally distinct from the surrounding hillslopes; (3) disrupted low-order drainage networks; and (4) visible vertical displacement of distinct stratigraphic units. Landslide perimeters were captured through heads-up digitizing in ArcMap and included both deposit and source area. Crosscutting relations were used wherever possible to constrain landslide boundaries, but in places, these could not be discerned, and boundaries within some continuous complexes were somewhat arbitrarily located. We also independently assessed landslide occurrence for all areas mapped as "Qls" (Quaternary landslide deposit) on the 1:500,000 geologic map of Oregon (Walker and MacLeod, 1991).

There is mapping error associated with our effort. Inevitably, not all true landslides were mapped while some nonlandslide features were mapped. All catchments were mapped with the same degree of scrutiny of remote imagery of comparable quality. We therefore believe that landslide mapping errors are relatively evenly distributed, introducing noise but little systematic bias into our analyses. To supplement remote mapping, we field-checked ~15% of remotely mapped landslides. This provided useful checks on landslide designations, particularly in forested terrain, where vegetation mutes hummocky topography and obscures displaced stratigraphic contacts.

The distribution of mapped landslides is shown in Figure 1. A digital version of the landslide map is contained in the GSA Data Repository (ESRI Shapefile).[1] Approximately 90% of these lie within a NW-SE–trending band, ~50–100 km wide, that originates in the SE corner of Oregon and terminates ~30 km SE of Mount Hood. The remaining landslides are concentrated in the southern portion of the study area along topographic features associated with Basin and Range structures.

Figure 2 shows the size distribution of the mapped landslides. Over 400 landslides were mapped, ranging in area from ~0.1 km^2 to ~40 km^2. Approximately one third of the landslides are <1 km^2 in area, while half are between 1 and 5 km^2. Each basin has over 85 landslides: the Deschutes River basin has the most (127), and the John Day River basin has the highest concentration (~5×10^{-3} slides/km^2). Each basin contains landslide complexes >5 km^2.

The majority of mass movements mapped are multiple rotational slides, though many are complex. Approximately 5%–10% are lateral spreads, earth flows, or debris flows (Varnes, 1978).

To our knowledge, age constraints are available for only ~5% of mapped slides. Badger and Watters (2004) dated the Punchbowl slide on Winter Ridge to early to mid-Holocene, while Foster Creek and Bennett Flat slides are both older than 16.8 ka and younger than several 100 ka in age. Along the Deschutes River, Beebee (2003) dated one of the Whitehorse Rapids slides to between ca. 38 and ca. 65 ka, while showing that three other adjacent features are younger. A giant debris flow at Dant postdates a Mount Jefferson eruption that likely occurred between 74 and 59 ka (O'Connor et al., 2003). In the John Day River basin, one of the mapped landslides formed a natural dam ca. A.D. 1800, creating Lake Magone. Near the base of sediments filling closed depressions on several landslides in the Deschutes, John Day, and Owyhee River basins, we found confirmed or suspected Mount Mazama tephra, indicating slide ages of >7.7 ka. These landslides are associated with Boxcar and Wapinitia Rapids; Burnt Ranch Rapids; and Artillery Rapids on the Deschutes, John Day, and Owyhee Rivers, respectively. The Artillery Rapids slide toe is onlapped by debris from a younger landslide originating across the river. Two landslides immediately downstream are of Pleistocene age, mantled by gravel likely deposited behind the West Crater lava dam, which persisted until at least 47.2 ka (Orem et al., 2009). The toes of at least four mapped slides on Owyhee River tributary Bogus Creek appear to be buried by, and thus older than, the West Crater lava flow, which is 60–90 k.y. old (Brossy, 2007; Brossy et al., 2008). In a subsequent section, we describe evidence for landslides ranging in age from ca. 10 ka to ca. 100 ka at the Hole in the Ground reach of the Owyhee River.

In summary, each drainage basin contains numerous large, predominantly rotational landslides, which collectively exhibit a distinct pattern. Although age data are sparse, they indicate that failures are primarily early Holocene and older. To interpret the pattern of landslides, we examined spatial associations between landslides and possible controls on their occurrence.

CONTROLS ON REGIONAL LANDSLIDE DISTRIBUTION

While previous research in the study area has not emphasized regional patterns of landslide distribution, geologic maps have included landslide designations (cf. Ma et al., 2009), and individual occurrences of large landslide complexes have been described (e.g., Carter, 1998;

[1]GSA Data Repository item 2011017, a shapefile of the mapped landslides, is available at http://www.geosociety.org/pubs/ft2011.htm or by request to editing@geosociety.org.

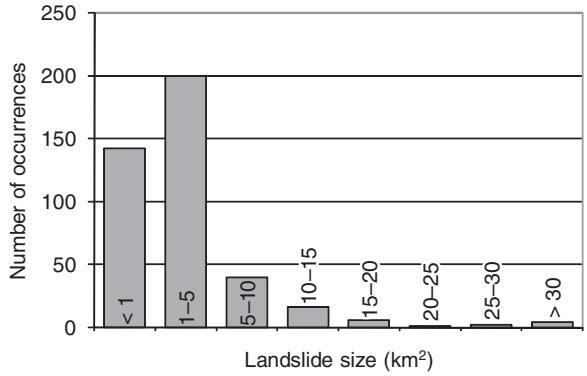

Figure 2. Frequency distribution of mapped landslide areas. Note that intervals on *x*-axis are not equal.

Beebee, 2003; O'Connor et al., 2003; Badger and Watters, 2004). Our geospatial analyses focused primarily on the regional importance of lithologic and stratigraphic controls on landslide occurrence. We sought to contextualize those controls relative to other potentially important controls on landslide occurrence, such as topography, which provides the fundamental impetus for mass movement, and structures (faults, folds), which may deform and weaken rocks locally. The relative importance of each of these controls has implications for future patterns of landsliding and therefore landscape evolution.

Lithology and Stratigraphy

To determine the importance of lithologic and stratigraphic controls on landslide distribution, we first identified the rock types involved in each mapped landslide. We buffered each landslide polygon and intersected the buffered polygons with the 1:500,000 scale digital geologic map of Oregon (Walker et al., 2002). The rock types captured by each buffered polygon were then identified.

Buffers were used to extend landslide polygons for two reasons. First, they compensated for contact boundary location error, which we estimated at 0.5–1 km. Second, previously mapped landslides are identified as Qls on the geologic map. Where our mapping coincided with preexisting Qls designations, buffering captured information about surrounding rock types. To limit inequalities in buffer area relative to landslide area, we scaled buffer width logarithmically with landslide area. Buffer width varied from 0.65 km for 0.1 km^2 polygons to 1.1 km for the largest polygon (nearly 40 km^2), with polygons of ~1 km^2 employing a 1 km buffer.

Although a compilation of higher-resolution digital geologic maps has now become available for Oregon (Ma et al., 2009), we used the 1:500,000 scale digital map because: (1) spatial coverage of the 1:500,000 scale map was more extensive than the compilation when our work was undertaken; (2) naming inconsistencies across map sheets and the vast number of rock units in the compilation hindered identification of broad patterns; and (3) the broad similarity of mapped landslide locations across the two data sets suggested that the state geologic map could adequately represent first-order relationships. Since digital geologic data sets consistent in both scale and classification scheme were not available for adjacent states, 25 landslides that fell outside the state borders of Oregon were excluded from spatial analyses involving rock type. We do not believe this exclusion influenced our overall results, given the small number of landslides involved.

Figure 3 shows the rock types most commonly involved in landslides throughout the study region. Rock types have been broadly classified into "coherent" or "weak" units based on the dominant character of each as inferred from unit descriptions and/or from qualitative assessments made in the field. For example, rocks of the Columbia River Basalt Group (e.g., Tc, Table 1) were considered coherent, while volcaniclastic fluviolacustrine sediments prevalent in the Owyhee River basin (e.g., Tlf, Table 1) were classified as weak. Our unit classifications are broad, and the character of the rocks within them varies spatially. Figure 3 illustrates that both coherent and weak rocks occur with high frequency in the landslides mapped. Approximately 80% of mapped, buffered landslides contain at least one coherent and one weak rock type.

To explore the notion that the co-occurrence of coherent and weak rocks may exert an important control on landslide distribution, we analyzed the frequency with which each rock type pairing occurred within buffered landslide polygons. Sixteen rock-type combinations, excluding those containing Qls, that occurred within 20 or more landslides were earmarked for further analysis (see following; Table 1A). In addition, for all rock-type pairs, we divided the number of times each rock-type pair occurred in a landslide by the number of times each individual rock type in that pair occurred in a landslide. This helped identify three additional potentially important stratigraphic sequences involving spatially sparse rock types (Table 1A). Of the 19 rock-type pairs examined, 14 included a coherent and a weak unit (Table 1B).

We hypothesized that the exposure of "key contacts" between coherent and weak rock types is a dominant factor in localizing landslides. To test this hypothesis, we created a polyline shapefile for each of the 19 abundantly occurring rock-type pairs. Each shapefile contained the plan-view pattern of contact between the two rock types. We then applied a 1 km buffer to each key contact pattern, creating 19 new shapefiles of strip-shaped polygons. Each polygon layer was then intersected with the unbuffered, mapped landslides (Fig. 4). The percentage areal overlap between each set of buffered key contact polygons and mapped landslide polygons was determined. This highlights the association of each contact with landslides, normalized by the overall prevalence of each contact. In some places, large landslides obscure key contacts (Fig. 4), and the analysis underestimates the strength of the association.

Figure 5 summarizes the results of the key contact analyses. The contacts exhibit a 25-fold variation in landslide involvement. The key contacts with the weakest association with landsliding are those between "Qal" (Quaternary alluvium) and other rock types, both coherent and weak. This finding is unsurprising, because Qal is most often a superficial deposit mantling the underlying bedrock governing failure mechanics, but we included it in case old alluvium layers between coherent rocks localized landslide failure surfaces. If pairs that involve Qal are excluded, the contacts exhibit an 8-fold variation in landslide involvement. Three contacts stand out as the most significantly associated with landslides, each of which has ~6% areal overlap between buffered contacts and mapped landslides: Tc-Tsfj, Tcg-Tsfj, and Tb-Tlf. Each is a contact between a coherent and a weak rock unit, and each is two to three times more commonly associated with landslides than the average association for all the potential key contacts examined.

The frequency with which pairs of weak and coherent rock types occur in landslides and the strong association of select pairs of weak and coherent rock types with landsliding suggest that rock strength contrast is indeed an important control on landslide occurrence. This hypothesis is further supported if the weak rocks lie beneath the coherent rocks, as landslide failure planes are commonly localized in the

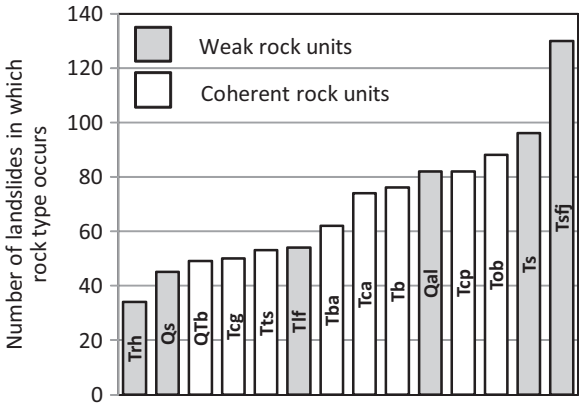

Figure 3. The most common rock types found in buffered landslide polygons. Individual landslides may contain multiple rock types. Both "coherent" and "weak" rock types (see text) occur with high frequency in and around landslides. Codes are explained in Table 1.

TABLE 1A. ROCK-TYPE PAIRS DESIGNATED AS "KEY CONTACTS"

Qal-Tb	Tba-Tts	Tb-Qs	Tca-Tct	Tca-Tsfj
Qal-Tts	Tba-Tob	Tb-Tlf	Tob-Tb	Tcg-Tsfj
Qal-Qs	Tc-Tsfj	Tb-Tts	Tob-Tlf	Tcp-Tsfj
Qal-Tba	Tr-Tsfj	Tca-Tcp	Tob-Ts	

TABLE 1B. BRIEF DESCRIPTIONS OF ROCK TYPES INVOLVED IN DESIGNATED "KEY CONTACTS"

Code	Rock type	Description	Relative strength designation
Qal	Alluvial deposits	Sand, gravel, and silt forming floodplains and filling channels of present streams. In places includes talus and slope wash.	Weak
Tb	Basalt	Basalt flows, flow breccia, and basaltic peperite; minor andesite flows.	Coherent
Tts	Tuffaceous sedimentary rocks, tuffs, pumices, and silicic flows	Moderately well-indurated lacustrine and fluvial (floodplain) deposits of tuff, pumicite, palagonite tuff, and lesser siltstone, arkosic sandstone, and pebble and cobble conglomerate.	Weak
Qs	Lacustrine and fluvial sedimentary rocks	Unconsolidated to semiconsolidated lacustrine clay, silt, sand, and gravel.	Weak
Tba	Basalt and andesite	Lava flows and breccia of aphyric and plagioclase porphyritic basalt and aphyric andesite.	Coherent
Tob	Olivine basalt	Thin, commonly open-textured (diktytaxitic), subophitic to intergranular olivine basalt flows.	Coherent
Tsfj	Rhyolitic tuff, tuffaceous sedimentary rocks, and lava flows	Rhyolitic to dacitic varicolored bedded tuff, lapilli tuff, and fine- to medium-grained tuffaceous sedimentary rocks with interstratified welded and nonwelded ash-flow tuff and interbedded basalt and andesite flows.	Weak
Tc	Columbia River Basalt Group and related rocks	Subaerial basalt and minor andesite lava flows and flow breccia and minor palagonitic tuff and pillow complexes of the Columbia River Basalt Group.	Coherent
Tr	Rhyolite and dacite domes and flows	Mostly light-gray to red, dense, flow-banded, nonporphyritic and porphyritic rhyolite and dacite in nested domes, small intrusive bodies, and related flows.	Coherent
Tlf	Lacustrine and fluvial deposits	Poorly to moderately consolidated, bedded silicic ash and pumicite, diatomite, tuffaceous sedimentary rocks, minor mudflow deposits, and some coarse epiclastic deposits.	Weak
Tct	Predominantly tuffaceous facies of Clarno Formation	Mapped separately by Swanson (1969a) in the Ochoco and Maury Mountains of the Blue Mountains Province.	Weak
Tcp	Picture Gorge Basalt	Flows of aphyric and plagioclase porphyritic flood basalt.	Coherent
Tca	Clastic rocks and andesite flows	Mostly andesitic lava flows, domes, breccia, and small intrusive masses and lesser basaltic to rhyolitic rocks.	Coherent
Tcg	Grande Ronde Basalt	Flows of dark-gray to black, aphyric tholeiitic basalt.	Coherent
Ts	Tuffaceous sedimentary rocks and tuffs	Semiconsolidated to well-consolidated fluvial or lacustrine tuffaceous sandstones, siltstones, mudstones, and conglomerates, plus palagonitic tuffs and tuff breccias.	Weak

Note: Excerpted from: http://nwdata.geol.pdx.edu/OR-Geology/explanation_dcp5.php?unit_id=Tb&Lookup=Lookup+code (accessed 11 June 2010).

weak rocks (e.g., Badger and Watters, 2004). We performed a spatial analysis to determine whether this was the case in our mapped landslides. First, we clipped the digital geologic map with the buffered landslide polygon layer. This created a layer containing geologic information only in the interior of the buffered landslide polygons. Each buffered landslide polygon contained several smaller polygons of rock types. Next, we determined the average elevation of each rock-type polygon within each landslide polygon by performing a zonal analysis on the mosaic 10 m DEM, with each zone defined as a rock-type polygon. We then calculated the mean elevation of the mean elevations of all the coherent rock-type polygons in each landslide. We did the same for all of the weak rock-type polygons and subtracted the latter from the former.

Figure 6 shows the results of the rock-type elevation analysis. Landslides containing only coherent or only weak rock types were excluded from Figure 6, as were Qal and Qls polygons. Figure 6 indicates that, for a clear majority of landslides analyzed (75%), coherent rock types occurred topographically, and presumably stratigraphically, above weak rock types. Hence, the presence of coherent rocks on top of weak rocks is strongly associated with landsliding in central and eastern Oregon.

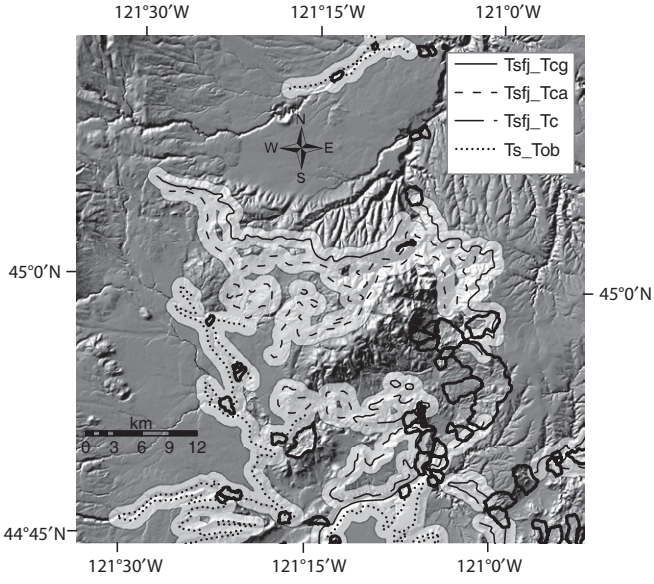

Figure 4. Example location on lower Deschutes River showing relationship of mapped landslides (heavy black outline) to key contacts (see Table 1) surrounded by a 1 km buffer (semitransparent polygons). Percent areal overlap between each of the buffered contacts and the mapped landslides is shown in Figure 5. Mapped features are draped over a shaded relief rendering of a 1 arc s digital elevation model (DEM).

Topography

Fundamentally, landsliding is driven by potential energy gradients dominated by local elevation differences, so topography should partially explain the distribution of landslides. To examine this link, we created a "local relief" grid from the 10 m DEM mosaic. The value within each grid cell was the maximum minus minimum elevation within a circular neighborhood of 1 km diameter centered on the cell. This essentially reflects gradient over a half-valley width, a scale to which landsliding should be responsive. We then applied three thresholds,

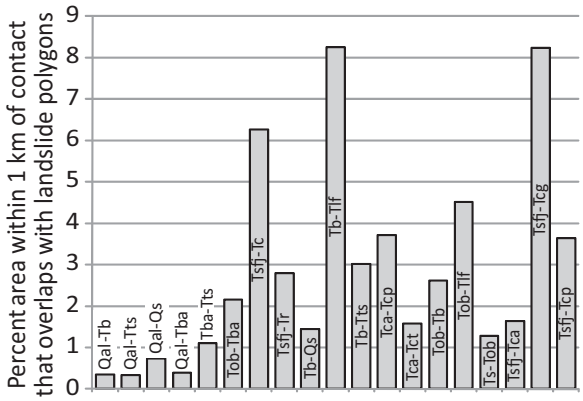

Figure 5. Percent of polygon area created by applying a 1 km buffer to each key contact that overlaps with mapped landslides. This process normalizes for contact prevalence and highlights the three contacts most strongly associated with landsliding.

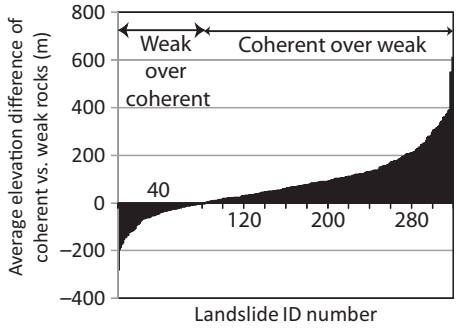

Figure 6. Elevation difference between average height of coherent rock types and average height of weak rock types within buffered slides containing both rock types.

60 m, 100 m, and 200 m, to the continuous local relief grid. Each subsampled grid was then turned into a polygon shapefile, with polygons representing patches of cells in the parent grid that contained values (as opposed to no data). Each polygon shapefile was then intersected with the shapefile containing the mapped landslides (Fig. 7). The percent overlap between the landslide data set and each local relief data set was then determined.

The results are shown in the dark-shaded bars of Figure 8. Landslides cover ~1% of the study area without regard to local relief and ~2.5% of the area with ≥200 m of local relief. To isolate further the effects of topography, the analysis was repeated on terrain >1 km from any of the key contacts. Landslides cover 0.7% of the study area that lies >1 km from any of the key contacts without regard to local relief. Increasing local relief increases this percentage, but the effect levels off with larger thresholds. Thresholds of 100 m and 200 m both create a roughly doubled association with landsliding, to 1.6% (Fig. 8). When the analysis is repeated on a subset of the terrain *within* 1 km of any key contact (e.g., Fig. 7), the effects of local relief on landslide prevalence are more notable. Approximately 2% of the study area lying within 1 km of a key contact is involved in landsliding, regardless of local relief, while landslides cover 6.3% of areas lying within 1 km of a key contact and supporting ≥200 m of local relief. The effect of local relief in proximity to key contacts becomes *more* pronounced with higher threshold values, the largest increase being between the 100 m and 200 m thresholds. Hence, topographic gradient is an important control on landslide distribution, and its contribution is most significant in proximity to key contacts.

Structure

A third category of possible controls on the distribution of landslides is structural features. We hypothesized: (1) that shattering of rock associated with faulting promotes landsliding through local rock mass strength reduction; and (2) that folds promote landsliding through the creation of dip slopes. To examine the first hypothesis, we determined fault density (fault length per unit area) across the study region; within landslide polygons; and within landslide polygons extended by buffers of 0.3, 0.7, 1, and 2 km. Fault locations were obtained from version 4 of the Oregon Geologic Data Compilation (OGDC; Jenks et al., 2008), which contained the best digital fault mapping available at the time of analysis. This analysis was conducted over ~80% of the study region.

Figure 9 shows the results of the fault density analysis. Fault density within landslide polygons

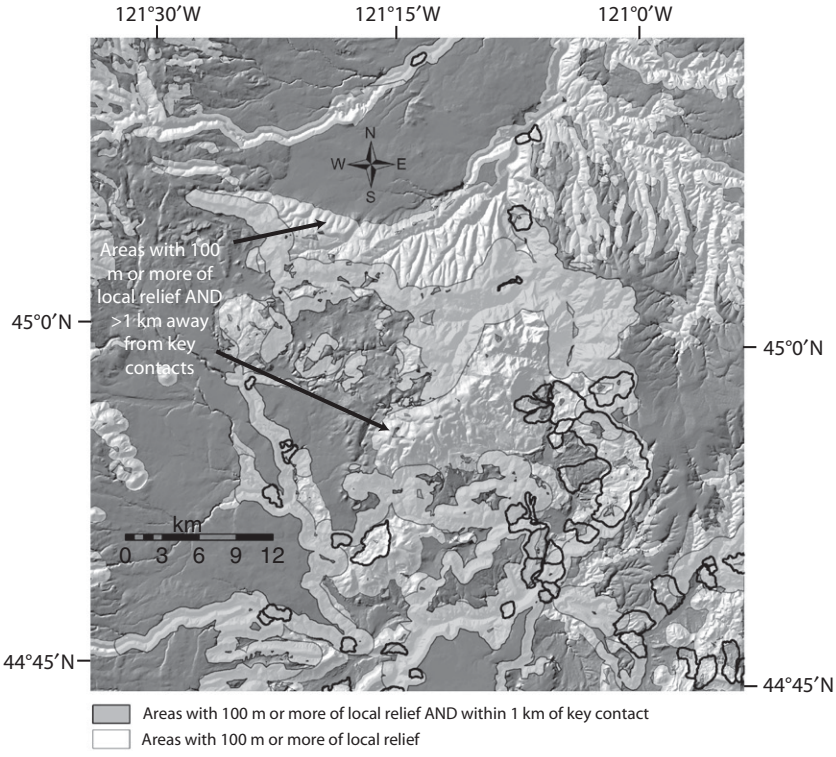

Figure 7. Example location on lower Deschutes River showing relationship of mapped landslides to distribution of areas exceeding one of the three local relief thresholds applied. Semitransparent white polygons indicate local relief >100 m. Semitransparent gray polygons indicate local relief >100 m within 1 km of a key contact. Where white and gray polygons do not overlap, terrain has local relief >100 m and is >1 km from a key contact.

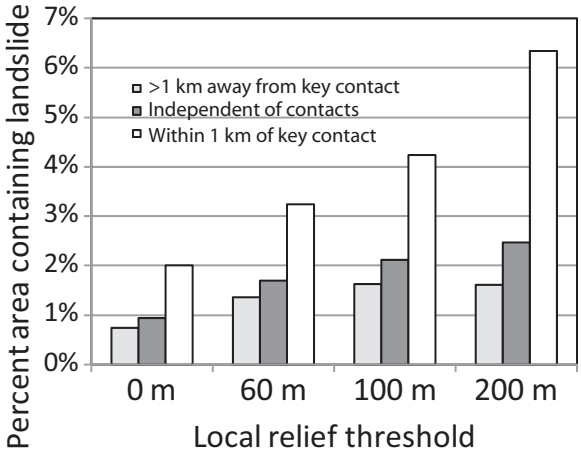

Figure 8. Percent areal overlap between mapped landslide polygons and portions of the landscape meeting local relief thresholds. Percent of total study area occupied by landslides is represented by the dark shaded bar with a 0 m threshold (i.e., no threshold) applied. The other dark shaded bars represent percent areal overlap between mapped landslides and portions of the landscape having ≥60 m, 100 m, or 200 m of local relief. Light shaded bars represent areal overlap between mapped landslides and terrain that: (1) meets each local relief threshold, *and* (2) is >1 km away from any key contact. White bars represent areal overlap between mapped landslides and terrain that: (1) meets each local relief threshold, *and* (2) is within 1 km of any key contact.

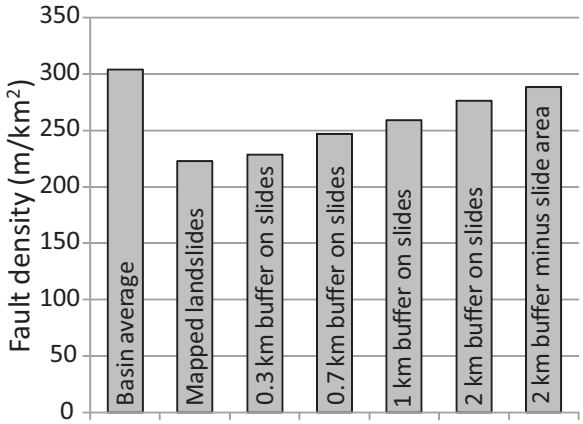

Figure 9. Fault density in: the whole study area, mapped landslides, and mapped landslides with specified buffers imposed. Overlapping buffer zones were merged to prevent double counting. The bar labeled "2 km buffer minus slide area" reflects the fault density only in the buffer ring around the landslide, not within the landslide itself. Fault data are from OGDC v. 4 (Jenks et al., 2008).

is ~25% lower than the basin-averaged fault density of ~300 m/km^2. This may partly reflect difficulty of mapping faults through landslide-disrupted terrain. Fault density increases with buffer width but is still below the basin-averaged value for a buffer width of 2 km. Fault density computed for the buffer zone only, exclusive of the landslide area, is ~290 m/km^2—close to, but still slightly lower than, the basin-averaged fault density. Overall, the analysis suggests that landslides are not concentrated in fault-ridden areas, and that bedrock shattering through faulting is not a major control on landslide distribution.

Possible linkages between landsliding and tilting of strata had to be examined indirectly, because digital strike and dip data do not yet exist for central and eastern Oregon. Limited digital data on fold axis locations were available at the time of analysis in version 2 of the OGDC (Jenks et al., 2006). This data set covered 50% of our study area, which contains 213 mapped landslides. Within that area, we performed a fold axis density analysis similar to the fault density analysis. We used buffers on mapped landslides with widths of 2, 3, 5, 10, 20, and 40 km. We also computed the distance between each mapped landslide in the analysis area and the nearest fold axis. We then compared that distribution of distances to one computed using an equal number of polygons randomly distributed throughout the analysis area.

Mapped folds are much sparser than mapped faults. Fold density averaged over the analysis area is less than 0.02 m/km^2 (Fig. 10A) and is slightly lower within 2–3 km of mapped landslides. However, fold density computed with a 10 km buffer on mapped landslides is ~40% greater than the average for the analysis area. One interpretation of this result is that regional folds are relatively broad, with dips that are gentle within 2 or 3 km of the fold axes but that steepen some 5–10 km away and die out >10 km away. The proximity analysis shows that similar numbers of mapped landslides and randomly distributed polygons occur within 3 km from fold axes (Fig. 10B), while ~50% more mapped landslides (~20 altogether, or 10% of landslides analyzed) fall within 3–10 km of fold axes than do randomly distributed polygons. This result suggests a spatial association between landslides and fold axes effective only over intermediate distances of several kilometers. In contrast, between 10 and 20 km from fold axes, there are 100% more randomly distributed landslides than mapped landslides. Half of mapped landslides are >20 km from any fold axis, suggesting that any inferred association between landsliding and folding likely excludes a significant subset of the landslides. Both folds and landslides are clustered within the analysis area (Fig. 11), but only some of the clusters overlap. Further exploration of these hypotheses awaits improved digital data sets of structural features.

In summary, lithologic and stratigraphic controls play a major role in the distribution of landslides in central and eastern Oregon. Landslides are strongly associated with lithologic contacts that juxtapose coherent rocks atop weak units. The strength of this linkage is strongly enhanced as topographic gradient increases, while increased topographic gradient alone has a more modest impact on landslide prevalence. Tilting of strata associated with folding may contribute to localizing ~10% of mapped landslides. Fault density does not appear to exert an important control on landslide distribution.

INTERPRETATION OF PRESENT LANDSLIDE DISTRIBUTION AND IMPLICATIONS FOR THE FUTURE

On the broadest scale, our findings assist with interpretation of the landslide distribution shown in Figure 1. Regional volcanic and tectonic histories set up the stratigraphic relations that strongly affect landslide occurrence and distribution in central and eastern Oregon. Tectonically disrupted drainage networks formed lake basins that filled with fine-grained fluviolacustrine sediments (e.g., Cummings et al., 2000). Volcanic activity from arc and vent systems spread volcaniclastic debris throughout much of the study area (e.g., Smith et al., 1989; Christiansen and Yeats, 1992). These relatively fine-grained and/or noncohesive materials were then capped by coherent lava flows, primarily basaltic in composition (e.g., Jordan et al., 2004; Camp and Ross, 2004). The widespread occurrence of these stratigraphic characteristics preconditioned much of the study

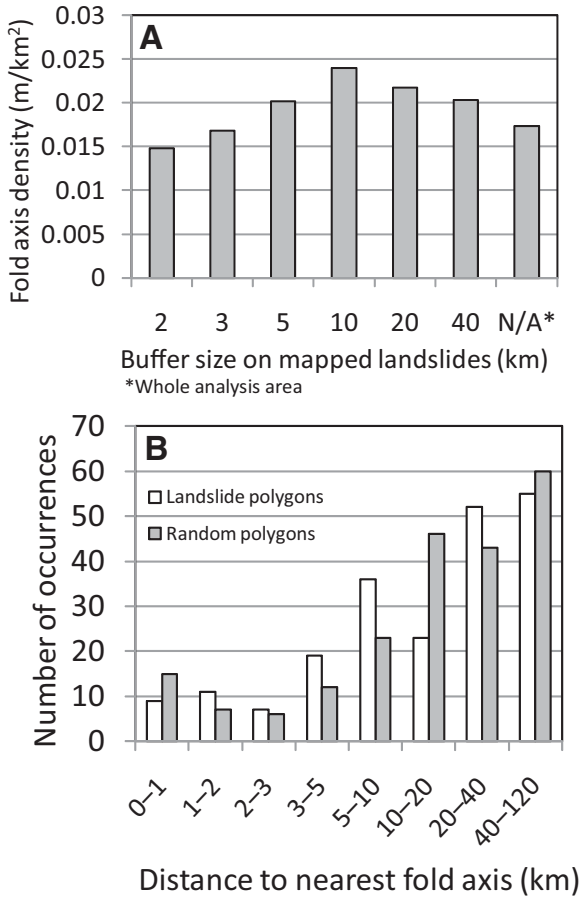

Figure 10. Quantitative relationship between landslide distribution and fold axis distribution. Analyses were restricted to ~50% of the study area (containing 213 landslides) for which fold axis data were available via OGDC v. 2 (Jenks et al., 2006). (A) Fold axis density in polygons defined by mapped landslides with specified buffer sizes surrounding them. Overlapping buffer zones were merged to prevent double counting. (B) Frequency distribution of distances from mapped landslides to nearest fold axis, compared to similar frequency distribution using randomly distributed landslides. Note that intervals along horizontal axis are unequal.

landscape for failure. This latent potential for landsliding appears to be realized wherever it is accompanied by sufficiently great topographic gradients, such as along the NW-SE–trending band in which most of the mapped landslides occur. Few landslides are found SW of this band, possibly because Pliocene–Quaternary basaltic volcanism affected a swath of the landscape along the Brothers fault zone, subparallel to the zone of high landslide concentration (Jordan et al., 2004; Camp and Ross, 2004). The infilling of local topography by effusive lavas effectively reduced local relief, and the geomorphic response to those volcanic events is still ongoing. Fluvial incision is a principal generator of local relief in the study region, but drainage network incision, and even integration, within the zone of most significant Pliocene–Quaternary volcanism is weak because: (1) local relief reduction occurred relatively recently; (2) the affected region is relatively dry; and (3) the region is far (100–200 km) from local base level—the Columbia and Snake Rivers. Only farther to the SW, where Basin and Range tectonics generate substantial local relief along discrete structures, do scattered landslides occur outside the zone of most intense fluvial dissection. The seismic activity associated with these range-bounding faults may also trigger and enlarge landslides (Badger and Watters, 2004).

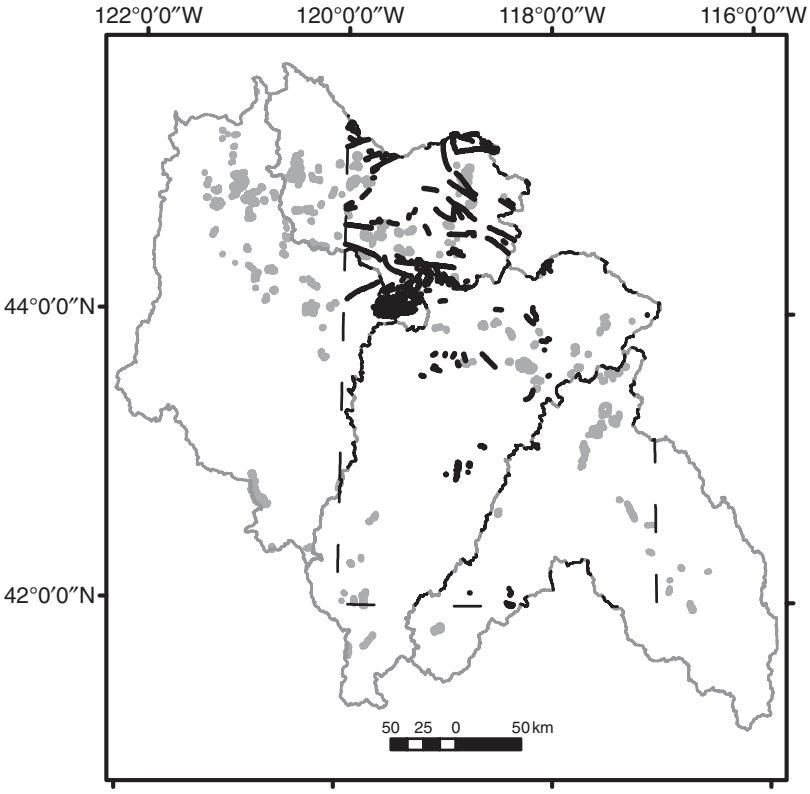

Figure 11. Distribution of fold axes contained in OGDC v. 2 (Jenks et al., 2006) and of mapped landslides. The dashed line indicates the extent of the area in which fold data were mapped. Thick black lines indicate fold axes. Thick gray polygon outlines delineate mapped landslides. Thin gray lines delineate basin boundaries.

To the NE of the prominent landslide zone, thick sequences of coherent basalt associated with the Columbia River Plateau and Snake River Plain curtail failure (Fig. 12). Beebee (2003) noted that landsliding along the Deschutes River is sparse wherever the valley walls consist entirely of Columbia River Basalt Group rocks, typically along the lower reaches of the river (Fig. 12A). This pattern appears to apply to the John Day River as well (Fig. 12B). As the Columbia River Basalt Group thins toward the south and the base of these rocks intersects the topographic surface, landsliding becomes evident. Landsliding produces canyon rim retreat and bouldery accumulations in the channel, e.g., at Clarno Rapids. The extent of landsliding increases upstream in these reaches. Assuming progressive landslide growth through time, this implies earlier initiation to the south (Fig. 12B).

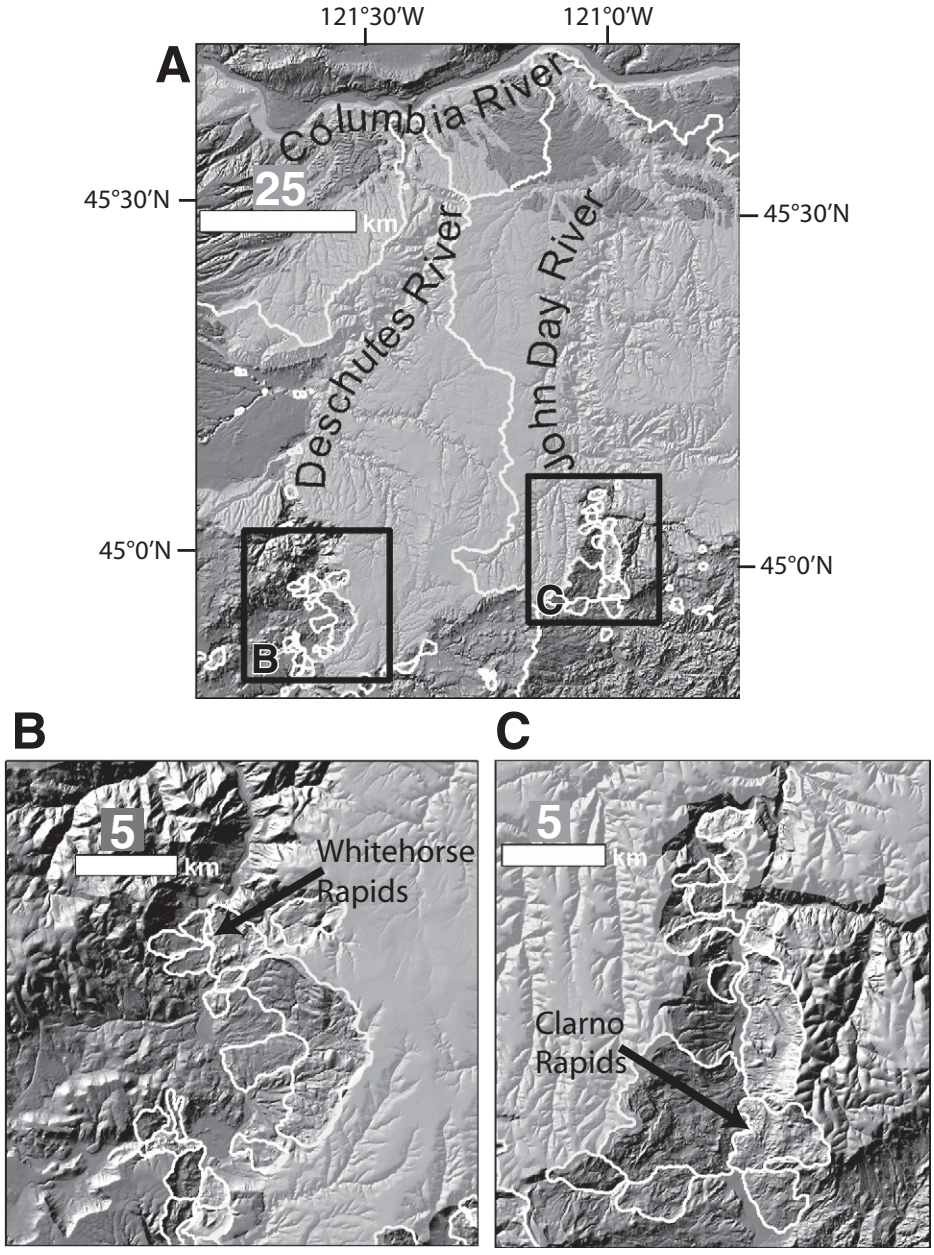

Figure 12. (A) Mapped landslides in the lower Deschutes and John Day Rivers. Mapped landslide polygons are outlined in white, as are basin boundaries. Light-gray overlay indicates extent of Columbia River Basalt Group (CRBG) in the region (Walker et al., 2002). Landslide abundance declines dramatically northward as the rivers enter thick sequences of Columbia River Basalt Group rocks (cf. Beebee, 2003). Close-up of: (B) lower Deschutes River; and (C) lower John Day River. Both Whitehorse Rapids (B) and Clarno Rapids (C) represent landslide lag deposits left after breached river blockages.

As incision of the region's trunk streams proceeds, landsliding will likely expand incrementally toward the NE. The rate of this expansion will depend on the topography at the base of the Columbia River Basalt Group and on the rate at which the lower reaches of these rivers incise. The overall thickening of the Columbia River Basalt Group toward the north, however, and the proximity of the lower reaches of the region's trunk streams to local base level suggest only limited and slow northward expansion of landsliding.

Toward the SW, significant expansion of landsliding should accompany drainage integration in the upper reaches of the fluvial network and incision into extensive areas stratigraphically preconditioned for failure. Where key contacts are exposed near present valley floors, continued channel incision should increase landslide susceptibility significantly (Fig. 8). Of course, landslide susceptibility will increase modestly everywhere that local relief increases. However, the locations of the most landslide-plagued reaches are pinned for periods of perhaps 10^5–10^6 yr by the spatial distribution of key stratigraphic sequences, a legacy of local tectonic and volcanic histories and their controls on surficial processes.

Reach-scale patterns of landsliding can feed back into regional patterns of channel network incision and therefore landscape evolution. Large landslides can create sharp local discontinuities in channel slope, width, bed character, and sediment supply (e.g., Hewitt, 1998, 2006; O'Connor et al., 2003; Korup, 2006) that can persist for 10^0 to 10^4 yr (e.g., Beebee, 2003; Brossy, 2007; Ouimet et al., 2007; Hewitt, 2006; Korup et al., 2010), fragmenting regional channel networks (e.g., Hewitt et al., 2008). They can also temporarily dam rivers or displace channels onto bedrock spurs (e.g., Hewitt, 1998; Korup, 2002, 2004; Ouimet et al., 2008). These perturbations can all impact local incision rates and therefore cumulative patterns of landscape evolution. For example, Ouimet et al. (2007) suggested that landsliding in the lower reaches of the Li Qui River in Sichuan, China, has significantly delayed the response of the Li Qui headwaters to rapid base-level fall on the Yalong River because of sediment accumulation and temporary incision cessation upstream of landslide dams. Conversely, landslide dams that breach catastrophically can potentially promote incision locally (e.g., Howard and Dolan, 1981; O'Connor et al., 2003). Such dams have formed and breached in the study area (O'Connor et al.,

2003; Beebee, 2003; Othus, 2008), but their net impacts on channel incision depend in part on dam longevity (Ouimet et al., 2007; Safran et al., 2008), which remains unquantified to date. However, spatial clustering of landslides and landslide dams may also significantly influence overall channel character (e.g., O'Connor et al., 2003) and long-term channel incision patterns (Safran et al., 2008). The stratigraphic controls on landslide occurrence that we document here are an important cause of long-lived spatial clustering.

A factor that contributes to the persistence of landsliding in a given area is cross-valley interaction among landslides. Many channel segments exhibit landsliding on both sides of the valley, with morphologic evidence suggesting more recent activity on one side or the other. By deflecting channels and causing undercutting of the opposing valley wall, landslides on one side of a valley may trigger subsequent landslides on the other side. Blockage potential and delivery of large-caliber debris can then persist until sources on both sides of the river are exhausted.

One reach that clearly exhibits a cross-valley disparity in landsliding age and a long history of landsliding is Hole in the Ground on the Owyhee River, ~25 km upstream from the western end of Lake Owyhee (Fig. 13). There, a particularly thick exposure (~900 m; Othus, 2008) of fine-grained, Tertiary fluviolacustrine sediments lies beneath several tens of meters of capping basalt. The morphology of a cluster of landslides on the south side of the valley is smooth (Fig. 13). Field inspection reveals that the ancient landslide blocks are mantled with thick alluvial fans and colluvial aprons that bury the topography nearly to the crests of the failed blocks. Strong stage 3 carbonate soils are developed in these debris aprons. Elsewhere in the area, strong stage 4 to stage 5 carbonate soils are developed on fan surfaces graded to a 1.9 Ma intracanyon lava flow. These data suggest a middle Pleistocene to early late Pleistocene age for the alluvial and colluvial deposits on the south side of the valley, implying an even older age for the underlying landslides. In contrast, mass movements on the north side of the valley are distinctly hummocky or show clear shear zones (Fig. 13). Outburst flood deposits, tentatively dated at ca. 10 ka (Othus, 2008), are associated with a lobe of this landslide complex. Landslide ages are too sparse and ill-constrained to develop clear event sequences throughout the study region, but limited geochronologic evidence from other reaches (e.g., Artillery Rapids) also indicates persistent landsliding over tens of thousands of years within the space of a few kilometers.

Hole in the Ground may also suggest an evolution in landslide style that other reaches may experience in the future. The headscarps on the north side of the valley are collapsing in multiple rotational failures, with a spacing of ~100 m between the rubbly crests of failed blocks (Fig. 13). Rotational failures die out 1–1.5 km downslope from the headscarp. They do not impact the channel directly. The lower portion of the landslide complex contains little coherent rock and sheds large earthflows that debouche into, and occasionally block, the channel. The most obvious of these has a toe ~1 km wide (Fig. 13). Since ongoing incision presumably exposes increasingly thick sections of underlying weak sediments in areas that have served as long-lived local depocenters, we hypothesize that other reaches will experience similar shifts in mass movement type, from rotational failure to earthflow or debris flow, with possible attendant shifts in the nature of channel impacts. A systematic analysis of average and maximum particle sizes delivered by mass movements in the study area relative to the adjacent rivers' transport capacities and the consequences for local geomorphic behavior is one intriguing prospect for future work at larger scales.

We expect that landslide-mediated, reach-scale perturbations of channel processes will persist until valley slopes achieve stable angles. The largest landslide complexes approach

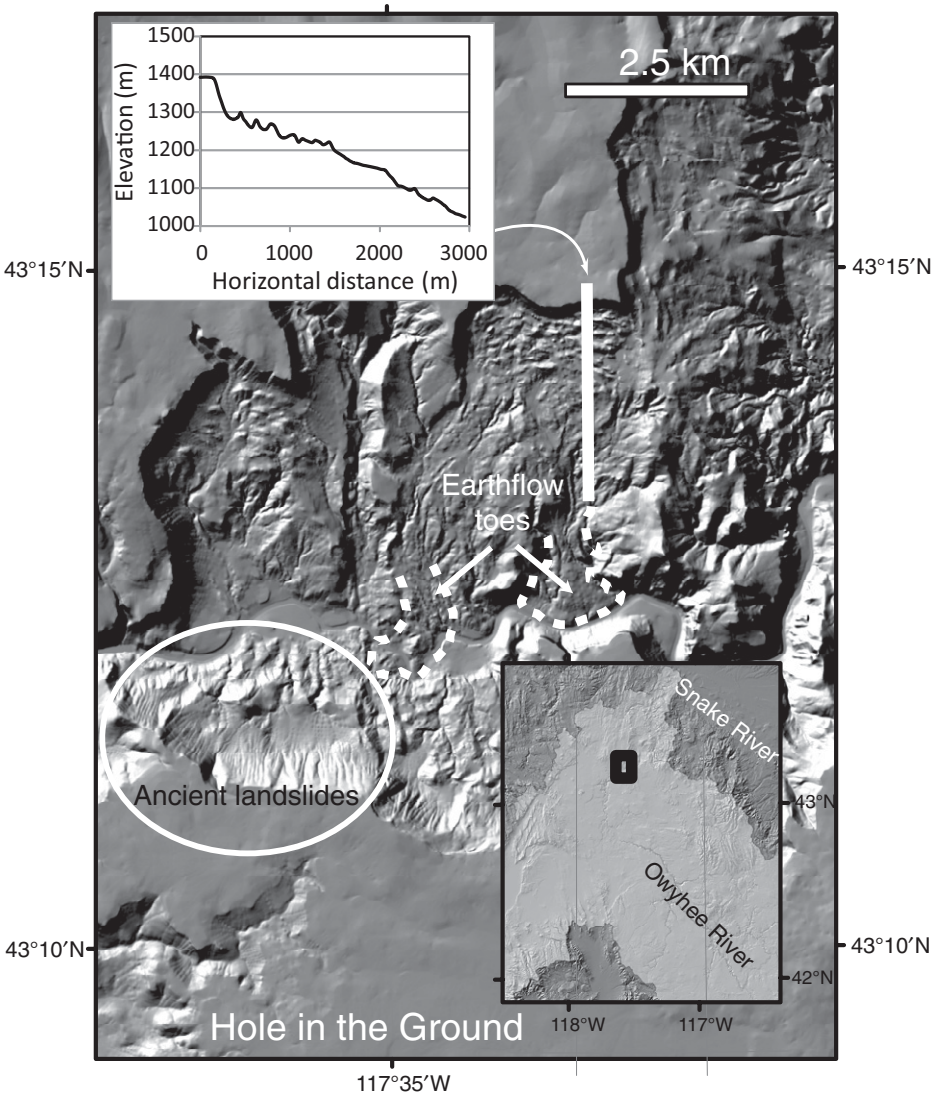

Figure 13. Landslide features at Hole in the Ground reach of the Owyhee River. Inset map shows location on the Owyhee River. The landslide complex exhibits fresh activity and diverse styles of mass movement on the north side. Landslides on the south side are more ancient, up to several hundred thousand years old.

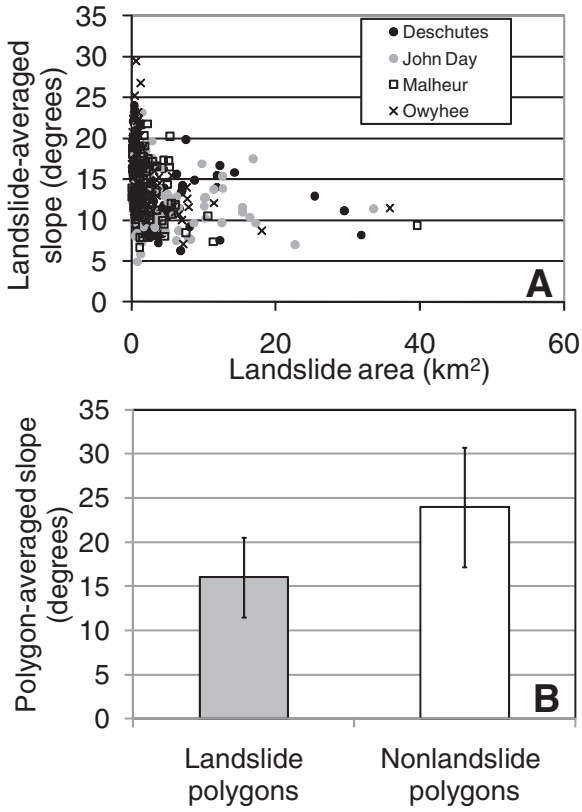

Figure 14. Effect of landsliding on valley wall slope. (A) Landslide-averaged slope as a function of landslide area. Landslide-averaged slope is the zonal average of local slopes, computed with the standard ArcMap algorithm, for all pixels within the landslide. For small landslides, the steep headscarp skews landslide-averaged slope toward high values. For landslides of ~20–40 km² area, landslide-averaged slope converges to 7°–13°, a value consistent with angles of internal friction for clays (Selby, 1993). (B) Comparison of polygon-averaged slope within 80 landslide polygons and 60 adjacent polygons drawn in the same lithologies along the main stem Owyhee River. Landslide slopes are ~8° less than are nonlandslide polygon slopes. Populations are statistically distinct (p = 0.05) based on a two-tailed t-test assuming unequal variances.

slopes of 7°–13° (Fig. 14A), similar to the angle of internal friction for clays (e.g., Selby, 1993). Landslides along the main stem Owyhee River create valley walls with slopes 8° lower on average than those of adjacent valley walls unaffected by landsliding with the same lithology (Fig. 14B). Progressive mass movement is therefore an important driver of interfluve evolution in large areas stratigraphically preconditioned for failure.

CONCLUSIONS

Over 400 large landslides and landslide complexes were mapped in central and eastern Oregon. Mapped landslides are concentrated in a NW-SE–trending swath 50–100 km wide, with scattered landslides also occurring along Basin and Range features. Landslide distribution is predominantly controlled by the coincidence of even modest local relief with the exposure of a few key contacts between weak sedimentary or volcaniclastic rock and more coherent cap rock. Fault density apparently exerts no control on landslide distribution, while ~10% of mapped landslides do appear to cluster within 3–10 km of mapped fold axes. Landslide occurrence is curtailed to the NE of the mapped distribution by thick packages of coherent basalt and to the SW by a lack of local relief. While ongoing incision and drainage integration may increase local relief throughout the region's valleys, our results suggest that future mass movements will be largely confined to areas stratigraphically preconditioned for failure by their volcanic, tectonic, and geomorphic histories. On the other hand, in such areas, landsliding may occur, at least episodically, over hundreds of thousands of years or more, impacting local channels with an evolving array of mass movement styles. The largest landslide complexes in this region of low relief result in valley wall slopes of ~7°–13°.

ACKNOWLEDGMENTS

This work was funded by the Geological Society of America's Gladys Cole Award; National Science Foundation grant EAR-617347; and John S. Rogers Summer Internship Program at Lewis & Clark College. The manuscript benefited from comments by Nancy Riggs, John Gosse, Kenneth Hewitt, and William Phillips. Shannon Othus spearheaded the first sustained look at two of the landslide-affected reaches on the Owyhee River. Jim O'Connor, Gordon Grant, and Robin Beebee provided stimulating exchanges about the impacts of large landslides on river valley evolution. The preliminary analyses of Lewis & Clark College's Spatial Problems in Geology class helped establish the scope and methodology of this project. This is the first publication of the Owyhee River Interstate Geologic Investigation Network.

REFERENCES CITED

Antinao, J.L., and Gosse, J., 2008, Large rockslides in the southern central Andes of Chile (32–34.5°S): Tectonic control and significance for Quaternary landscape evolution: Geomorphology, v. 104, p. 117–133, doi: 10.1016/j.geomorph.2008.08.008.

Badger, T.C., and Watters, R.J., 2004, Gigantic seismogenic landslides of Summer Lake basin, south-central Oregon: Geological Society of America Bulletin, v. 116, p. 687–697, doi: 10.1130/B25333.1.

Beebee, R.A., 2003, Snowmelt Hydrology, Paleohydrology, and Landslide Dams in the Deschutes River Basin, Oregon [Ph.D. dissertation]: Eugene, University of Oregon, 186 p.

Beranek, L.P., Link, P.K., and Fanning, C.M., 2006, Miocene to Holocene landscape evolution of the western Snake River Plain region, Idaho: Using the SHRIMP detrital zircon provenance record to track eastward migration of the Yellowstone hotspot: Geological Society of America Bulletin, v. 118, p. 1027–1050, doi: 10.1130/B25896.1.

Brossy, C.C., 2007, Fluvial Response to Intra-canyon Lava Flows, Owyhee River, Southeastern Oregon [M.Sc. thesis]: Ellensburg, Washington, Central Washington University, 110 p.

Brossy, C.C., Ely, L.L., House, P.K., O'Connor, J.E., Safran, E.B., Bondre, N., Champion, D.E., and Grant, G., 2008, The role of late Cenozoic lava flows in the evolution of the Owyhee River canyon, Oregon: Eos (Transactions, American Geophysical Union), v. 89, no. 53, Fall Meeting supplement, abstract H53B–1035.

Burns, W.J., Maidin, I.P., and Ma, L., 2008, Statewide Landslide Information Database for Oregon (SLIDO), Release 1: Portland, Oregon, Oregon Department of Geology and Mineral Industries, 26 p.

Camp, V.E., and Ross, M.E., 2004, Mantle dynamics and genesis of mafic magmatism in the intermontane Pacific Northwest: Journal of Geophysical Research, v. 109, p. B08204, doi: 10.1029/2003JB002838.

Carter, B.H., 1998, Safety of dams modification to Ochoco Dam Crooked River Project, Oregon: Proceedings of the Symposium on Engineering Geology and Geotechnical Engineering, v. 33, p. 25–36.

Carter, D.T., Ely, L.L., O'Connor, J.E., and Fenton, C.R., 2006, Late Pleistocene outburst flooding from pluvial Lake Alvord into the Owyhee River, Oregon: Geomorphology, v. 75, p. 346–367, doi: 10.1016/j.geomorph.2005.07.023.

Christiansen, R.L., and Yeats, R.S., 1992, Post-Laramide geology of the U.S. Cordilleran region, in Burchfiel, B.C., Lipman, P.W., and Zoback, M.L., eds., The Cordilleran Orogen; Conterminous U.S.: Boulder, Colorado, Geological Society of America, The Geology of North America, v. G-3, p. 261–406.

Costa, J.E., and Schuster, R.L., 1988, The formation and failure of natural dams: Geological Society of America Bulletin, v. 100, p. 1054–1068, doi: 10.1130/0016-7606(1988)100<1054:TFAFON>2.3.CO;2.

Crozier, M.J., 2010, Landslide geomorphology: An argument for recognition: Geomorphology, v. 120, p. 3–15, doi: 10.1016/j.geomorph.2009.09.010.

Cummings, M.L., 1991, Geology of the Deer Butte Formation, Malheur County, Oregon; faulting, sedimentation and volcanism in a post-caldera setting: Sedimentary Geology, v. 74, p. 345–362, doi: 10.1016/0037-0738(91)90072-L.

Cummings, M.L., Evans, J.G., Ferns, M.L., and Lees, K.R., 2000, Stratigraphic and structural evolution of the middle Miocene synvolcanic Oregon-Idaho graben: Geological Society of America Bulletin, v. 112, p. 668–682.

Evans, J.G., 1987, Geologic Map of the Owyhee Canyon Wilderness Study Area, Malheur County, Oregon: U.S. Geological Survey Miscellaneous Field Studies Map MF-1926, scale 1:62,500.

Ferns, M.L., Evans, J.G., and Cummings, M.L., 1993, Geologic Map of the Mahogany Mountain 30 × 60 Minute Quadrangle, Malheur County, Oregon, and Owyhee County, Idaho: Oregon Department of Mineral Industries Geologic Map Series GMS-78, scale 1:100,000, 1 sheet, 12 p. text.

Hasbargen, L.E., and Paola, C., 2000, Landscape instability in an experimental drainage basin: Geology, v. 28, p. 1067–1070, doi: 10.1130/0091-7613(2000)28<1067:LIIAED>2.0.CO;2.

Hermanns, R.L., and Strecker, M.R., 1999, Structural and lithological controls on large Quaternary rock avalanches (sturzstroms) in arid northwestern Argentina: Geological Society of America Bulletin, v. 111, p. 934–948, doi: 10.1130/0016-7606(1999)111<0934:SALCOL>2.3.CO;2.

Hewitt, K., 1998, Catastrophic landslides and their effects on the Upper Indus streams, Karakoram Himalaya, northern Pakistan: Geomorphology, v. 26, p. 47–80, doi: 10.1016/S0169-555X(98)00051-8.

Hewitt, K., 2006, Disturbance regime landscapes: Mountain drainage systems interrupted by large rockslides: Progress in Physical Geography, v. 30, p. 365–393, doi: 10.1191/0309133306pp486ra.

Hewitt, K., Clague, J.J., and Orwin, J.F., 2008, Legacies of catastrophic rock slope failures in mountain landscapes: Earth-Science Reviews, v. 87, p. 1–38.

Hovius, N., Stark, C.P., and Allen, P.A., 1997, Sediment flux from a mountain belt derived from landslide mapping: Geology, v. 25, p. 231–234, doi: 10.1130/0091-7613(1997)025<0231:SFFAMB>2.3.CO;2.

Hovius, N., Stark, C.P., Tutton, M.A., and Abbott, L.D., 1998, Landslide-driven drainage network evolution in a pre–steady-state mountain belt: Finisterre Mountains, Papua New Guinea: Geology, v. 26, p. 1071–1074, doi: 10.1130/0091-7613(1998)026<1071:LDDNEI>2.3.CO;2.

Howard, A.D., and Dolan, R., 1981, Geomorphology of the Colorado River in the Grand Canyon: The Journal of Geology, v. 89, p. 269–298, doi: 10.1086/628592.

Jenks, M.D., Niewendorp, C.A., Ferns, M.L., Staub, P.E., Lina Ma, and Geitgey, R.P., 2006, Oregon Geologic Data Compilation, Version 2: Portland, Oregon, Oregon Department of Geology and Mineral Industries.

Jenks, M.D., Wiley, T.J., Ferns, M.L., Staub, P.E., Lina Ma, Madin, I.P., Niewendorp, C.A., Watzig, R.J., Taylor, E.M., and Mertzman, S.A., 2008, Oregon Geologic Data Compilation, Version 4: Portland, Oregon, Oregon Department of Geology and Mineral Industries.

Jordan, B.T., Grunder, A.L., Duncan, R.A., and Deino, A.L., 2004, Geochronology of age-progressive volcanism of the Oregon High Lava Plains: Implications for the plume interpretation of Yellowstone: Journal of Geophysical Research, v. 109, p. B10202, doi: 10.1029/2003JB002776.

Korup, O., 2002, Recent research on landslide dams; a literature review with special attention to New Zealand: Progress in Physical Geography, v. 26, p. 206–235, doi: 10.1191/0309133302pp333ra.

Korup, O., 2004, Geomorphic characteristics of New Zealand landslide dams: Engineering Geology, v. 73, p. 13–35, doi: 10.1016/j.enggeo.2003.11.003.

Korup, O., 2006, Rock-slope failure and the river long profile: Geology, v. 34, p. 45–48, doi: 10.1130/G21959.1.

Korup, O., Strom, A.L., and Weidinger, J.T., 2006, Fluvial response to large rock-slope failures: Examples from the Himalayas, the Tien Shan, and the Southern Alps in New Zealand: Geomorphology, v. 78, p. 3–21.

Korup, O., Clague, J.J., Hermanns, R.L., Hewitt, K., Strom, A.L., and Weidinger, J.T., 2007, Giant landslides, topography, and erosion: Earth and Planetary Science Letters, v. 261, p. 578–589, doi: 10.1016/j.epsl.2007.07.025.

Korup, O., Densmore, A.L., and Schlunegger, F., 2010, The role of landslides in mountain range evolution: Geomorphology, v. 120, p. 77–90, doi: 10.1016/j.geomorph.2009.09.017.

Ma, L., Madin, I., Olson, K.V., and Watzig, R.J., 2009, Oregon Geologic Data Compilation, Version 5: Portland, Oregon, Oregon Department of Geology and Mineral Industries.

Malde, H.E., 1991, Quaternary geology and structural history of the Snake River Plain, Idaho and Oregon, *in* Morrison, R.B., ed., Quaternary Nonglacial Geology: Conterminous U.S.: Boulder, Colorado, Geological Society of America, Geology of North America, v. K-2, p. 251–281.

Mather, A.E., Griffiths, J.S., and Stokes, M., 2003, Anatomy of a 'fossil' landslide from the Pleistocene of SE Spain: Geomorphology, v. 50, p. 135–149, doi: 10.1016/S0169-555X(02)00211-8.

O'Connor, J.E., and Grant, G.E., eds., 2003, A Peculiar River—The Geology and Geomorphology of the Deschutes River, Oregon: American Geophysical Union, Water Science and Application Series 7, 210 p.

O'Connor, J.E., Curran, J.H., Beebee, R.A., Grant, G.E., and Sarna-Wojcicki, A., 2003, Quaternary geology and geomorphology of the lower Deschutes River canyon, Oregon, *in* O'Connor, J.E., and Grant, G.E., eds., A Peculiar River—Geology, Geomorphology, and Hydrology of the Deschutes River, Oregon: American Geophysical Union, Water Science and Application Series 7, p. 73–94.

Orem, C.A., Ely, L.L., House, P.K., Safran, E., and Brossy, C.C., 2009, Sedimentary record of two lava-dam impounded lakes, Owyhee River, southeastern Oregon: Geological Society of America Abstracts with Programs, v. 41, no. 7, p. 178.

Orr, E.L., and Orr, W.N., 1999, Geology of Oregon (5th ed.): Dubuque, Iowa, Kendall/Hunt Publishing Company, 254 p.

Othus, S.M., 2008, Comparison of Landslides and Their Related Outburst Flood Deposits, Owyhee River, Southeastern Oregon [M.Sc. thesis]: Ellensburg, Washington, Central Washington University, 136 p.

Ouimet, W.B., Whipple, K.X., Royden, L.H., Ziming Sun, and Ziliang Chen, 2007, The influence of large landslides on river incision in a transient landscape: Eastern margin of the Tibetan Plateau (Sichuan, China): Geological Society of America Bulletin, v. 119, p. 1462–1476.

Ouimet, W.B., Whipple, K.X., Crosby, B.T., Johnson, J.P., and Schildgen, T.F., 2008, Epigenetic gorges in fluvial landscapes: Earth Surface Processes and Landforms, v. 33, p. 1993–2009, doi: 10.1002/esp.1650.

Palmer, L., 1977, Large landslides of the Columbia River Gorge, Oregon and Washington: Reviews in Engineering Geology, v. 3, p. 69–83.

Palmquist, R.C., and Bible, G., 1980, Conceptual modeling of landslide distribution in time and space: Bulletin of the International Association of Engineering Geology, v. 21, p. 178–186, doi: 10.1007/BF02591559.

Philip, H., and Ritz, J.-F., 1999, Gigantic paleolandslide associated with active faulting along the Bogd fault (Gobi-Altay, Mongolia): Geology, v. 27, p. 211–214, doi: 10.1130/0091-7613(1999)027<0211:GPAWAF>2.3.CO;2.

Plumley, P.S., 1986, Volcanic Stratigraphy and Geochemistry of the Hole in the Ground Area, Owyhee Plateau, Southeastern Oregon [M.S. thesis]: Moscow, Idaho, University of Idaho, 161 p.

Reneau, S.L., and Dethier, D.P., 1996, Late Pleistocene landslide-dammed lakes along the Rio Grande, White Rock Canyon, New Mexico: Geological Society of America Bulletin, v. 108, p. 1492–1507, doi: 10.1130/0016-7606(1996)108<1492:LPLDLA>2.3.CO;2.

Repenning, C.A., Weasma, T.R., and Scott, G.R., 1995, The Early Pleistocene (Latest Blancan–Earliest Irvingtonian) Froman Ferry Fauna and History of the Glenns Ferry Formation, Southwestern Idaho: U.S. Geological Survey Bulletin 2105, Report B, 86 p.

Rib, H.T., and Liang, T., 1978, Recognition and identification, *in* Schuster, R.L., and Krizek, R.J., eds., Landslides, Analysis and Control: Washington, D.C., National Academy of Sciences, Transportation Research Board, Special Report 176, p. 34–80.

Roering, J.J., Kirchner, J.W., and Dietrich, W.E., 2005, Characterizing structural and lithologic controls on deep-seated landsliding: Implications for topographic relief and landscape evolution in the Oregon Coast Range, USA: Geological Society of America Bulletin, v. 117, p. 654–668, doi: 10.1130/B25567.1.

Safran, E.B., Peden, J.D., Harrity, K., Anderson, S.W., O'Connor, J.E., Wallick, R., House, P.K., and Ely, L., 2008, Impacts of landslide dams on river profile evolution: Eos (Transactions, American Geophysical Union), v. 89, no. 53, Fall Meeting supplement, abstract H54D–03.

Selby, M.J., 1993, Hillslope Materials and Processes (2nd ed.): Oxford, UK, Oxford University Press Inc.

Smith, G.A., 1986a, Simtustus Formation: Paleogeographic and stratigraphic significance of a newly defined Miocene unit in the Deschutes basin, central Oregon: Oregon Geology, v. 48, p. 63–72.

Smith, G.A., 1986b, Stratigraphy, Sedimentology, and Petrology of Neogene Rocks in the Deschutes Basin, Central Oregon: A Record of Continental-Margin Volcanism and its Influence on Fluvial Sedimentation in an Arc-Adjacent Basin [Ph.D. thesis]: Corvallis, Oregon State University, 464 p.

Smith, G.A., Bjornstad, B.N., and Fecht, K.R., 1989, Neogene terrestrial sedimentation on and adjacent to the Columbia Plateau; Washington, Oregon, and Idaho, *in* Reidel, S.P., and Hooper, P.R., eds., Volcanism and Tectonism in the Columbia River Flood-Basalt Province: Geological Society of America Special Paper 239, p. 187–198.

Van Tassell, J., Ferns, M., McConnell, V., and Smith, G.R., 2001, The mid-Pliocene Imbler fish fossils, Grande Ronde Valley, Union County, Oregon, and the connection between Lake Idaho and the Columbia River: Oregon Geology, v. 63, p. 77–84, 89–96.

Varnes, D.J., 1978, Slope movement types and processes, *in* Schuster, R.L., and Krizek, R.J., eds., Landslides, Analysis and Control: Washington, D.C., National Academy of Sciences, Transportation Research Board, Special Report 176, p. 11–33.

Walker, G.W., and MacLeod, N.S., 1991, Geologic Map of Oregon: Reston, Virginia, U.S. Geological Survey, scale 1:500,000.

Walker, G.W., MacLeod, N.S., Miller, R.J., Raines, G.L., and Connors, K.A., 2002, Spatial Digital Database for the Geologic Map of Oregon: U.S. Geological Survey Open-File Report OF-03-0067, 22 p.

Wood, S.H., and Clemens, D.M., 2002, Geologic and tectonic history of the western Snake River Plain, Idaho and Oregon, *in* Bonnichsen, B., White, C.M., and McCurry, M., eds., Tectonic and Magmatic Evolution of the Snake River Plain Volcanic Province: Idaho Geologic Survey Bulletin 30, p. 69–103.

Manuscript Received 1 March 2009
Revised Manuscript Received 15 January 2010
Manuscript Accepted 13 April 2010

Printed in the USA